

UDC 628

DOI: 10.15587/1729-4061.2021.224219

*The need to increase the ability of water hyacinth composites as EMI radar protection is related to the carbonization process of organic materials. This research aimed to determine the effect of water hyacinth carbonization temperature on the effectiveness of fabrication and EMI shielding radar. The research method includes the preparations such as cutting, washing, and drying the water hyacinth. The drying process is carried out using an oven with a temperature of 70 °C for 4 days. Then the water hyacinth is mashed until it reaches the 80 mesh size. Then the carbonization process is carried out, with variations in carbonization temperature ranging from 500 °C, 600 °C, 700 °C, 800 °C, 900 °C and 1,000 °C, with a heat increase speed of 3 °C/minutes. After reaching the specified temperature, a holding time is then carried out for 1 hour. Furthermore, the composite composition of 30 % water hyacinth activated carbon powder and 70 % phenol-formaldehyde (PF) resin was molded using a hot press with a pressure of 300 kg/cm<sup>2</sup> at 180 °C for 10 minutes. The results showed that the water hyacinth composite could be used as an EMI protection material at the X-Band frequency (8–12.5 GHz). Where the electrical conductivity and EMI SE increases with increasing carbonization temperature. Water hyacinth composites at a carbonization temperature of 1,000 °C showed the highest electrical conductivity and the highest EMI SE, respectively 4.64·10<sup>-2</sup> S/cm and 41.15 dB (attenuation 99.99 %) at a frequency of 8 GHz. The high absorption contribution is associated with the synergy combination of KCl and the pore structure of the goitre. KCl contributes to the magnetic properties and pore structure with high electrical conductivity values*

**Keywords:** carbonization temperature, water hyacinth, EMI shielding radar, holding time

# AN ANALYSIS OF EFFECT OF WATER HYACINTH CARBONIZATION TEMPERATURE ON FABRICATION AND EMI SHIELDING RADAR

**Azam Muzakhim Imammuddin**

Staf Pengajar

Program Studi Teknik Telekomunikasi

Departement of Electrical Engineering

State Polytechnic of Malang

Jl. Soekarno-Hatta, 9, Malang, Indonesia, 65141

Student of Mechanical Engineering Doctoral Program\*

E-mail: azam172.am@gmail.com

**Sudjito Suparman**

PhD, Professor\*\*

E-mail: sudjitospn@ub.ac.id

**Wahyono Suprpto**

PhD, Professor\*

E-mail: wahyos@ub.ac.id

**Achmad As'Ad Sonief**

Doctor of Engineering Sciences\*\*

E-mail: sonief@ub.ac.id

\*Departemen of Mechanical Engineering

Brawijaya University

Jl. Veteran, Ketawanggede, Kec. Lowokwaru,

Kota Malang, Jawa Timur, Indonesia, 65145

\*\*Department of Mechanical Engineering

Brawijaya University

Jl. Mayjend Haryono, 167, Malang, Indonesia, 65145

Received date 22.11.2020

Accepted date 26.01.2021

Published date 10.02.2021

Copyright © 2021 Azam Muzakhim Imammuddin, Sudjito Soeparman,

Wahyono Suprpto, Achmad As'ad Sonief

This is an open access article under the CC BY license (<http://creativecommons.org/licenses/by/4.0>)

## 1. Introduction

The need for polymer materials with various functions is increasing along with the development of nanotechnology today. The polymer is an ideal material in the industrial sector because it is very cheap, the production process is also relatively fast and the process is much simpler when compared to metal materials [1, 2]. However, it is very difficult to meet all the needs just relying on polymer alone. So it takes both organic and inorganic nanomaterials to get the desired properties. The combination of the polymer with the nanomaterial can improve the characteristics of the material [3–5]. This is in line with

the development of electronic devices/systems that require increasingly complex materials, with the hope of having a higher frequency range [4]. Many electronic components/devices are used at high frequencies, such as cell phones, satellite communications. The development of electronic device applications in the military, industrial and commercial sectors has created a new type of pollution known as sound or radio frequency interference (RFI) or electromagnetic interference (EMI) [5]. This interference can cause malfunction of devices, such as medical equipment, industrial robots, besides it can interfere with human health [6, 7]. Therefore, we need an effective protective material as a frequency damper [6, 7].

This protective material must have a high conductance. Currently, the protective material uses a metal coating material, which is used as EMI protection [8, 9]. However, the metal shields have disadvantages related to poor mechanical flexibility, weight, corrosion, whereas polymers have the advantage to overcome metal weaknesses [10]. So, conductive polymer composites with fillers such as metal particles, carbon particles, carbon fibers as EMI shields began to be used [11]. Meanwhile, among the fiber materials, which have the potential as EMI protection material are those that have a high aspect ratio. This is because it can increase the electrical conductivity of the low concentration resin matrix.

Electromagnetic waves are waves that do not need a medium to propagate. Electromagnetic waves can function as a carrier of electrical network waves, as a radio and television broadcast carrier, as a satellite communication information carrier, as a carrier for cellular communication information, useful in radar systems, and also as a source of energy [12].

Radio Detection and Ranging (RADAR) operates by emitting electromagnetic wave signals and detecting the reflection back from the target [13]. Targets can be aircraft, ships, spacecraft, vehicles, people, and the natural environment that reflects the return signal. Based on the reflected signal, the object's angle, distance, or velocity can be determined [14]. But sometimes the reflected signal cannot be detected. This could be because the radiation energy of the reflected signal is too small or absent due to being absorbed by the target. Targets that can absorb electromagnetic wave radiation are called anti-radar.

The mechanism of electromagnetic wave radiation protective materials includes: first, the wave reflection mechanism uses metal, this is because metals have electrons that are always moving [15]. Second, the absorption mechanism, where the material must have an electric or magnetic dipole, such as ZnO, SiO<sub>2</sub>, TiO<sub>2</sub>, BaTiO<sub>3</sub> for electric dipole materials or Fe<sub>2</sub>O<sub>3</sub>, Fe<sub>3</sub>O<sub>4</sub> for magnetic dipole materials [16]. Third, the double reflection mechanism, where this material has a large interface area and a porous structure such as a composite material containing a conductive filler material [17]. Meanwhile, the three types of EMI shielding materials are metals for reflection, conductive polymers for absorption or multi-reflection, and conductive composites for absorption or multi-reflection [18].

Several organic materials have been used as a basis for absorbing electromagnetic wave radiation. Where the material has a different carbon-hydrogen bond structure. So that when it is made into carbon, it will produce different crystal characteristics. Some agricultural waste is used as activated carbon, and functions as a protective material for EMI, including rice husks. This is because activated carbon is amorphous carbon [19].

In Indonesia, it is known to have abundant natural resources, where one of the potential natural ingredients to protect EMI is water hyacinth, which is found in swamps and rivers. Water hyacinth has three main components, namely cellulose, hemicellulose, and water hyacinth contains 50 % cellulose, 30 % lignin, the rest is hemicellulose and other substances. Also, water hyacinth has the property of easily absorbing heavy metals such as lead (Pb), copper (Cu), zinc (Zn), mercury (Hg), chrome (Cr), cadmium (Cd), manganese (Mn), iron (Fe) and sulfide compounds.

Therefore, based on the ingredients in water hyacinth, researchers need to conduct a study of the carbonization temperature of water hyacinth as a protective material for EMI radar. So that we find a method of making water hyacinth composites that can be used as an anti-radar material.

---

## 2. Literature review and problem statement

---

[20] using electromagnetic wave-absorbing materials provides additional materials that have metallic elements. Composite materials use a mixture of reduced graphene oxide (RGO), Fe<sub>2</sub>O<sub>3</sub> and carbon fiber (CF). The results of this study indicate that the content of Fe<sub>2</sub>O<sub>3</sub> greatly influences the absorption of electromagnetic wave radiation, with a maximum SE value of 45.26 dB. [21, 22] use carbon fiber and Fe<sub>2</sub>O<sub>4</sub> in composite form, with a composition of wt 5 % Fe<sub>2</sub>O<sub>4</sub>, 0.7 mm thickness and 8–12 GHz radar frequency with a maximum SE result of 67.9 dB. Another study used electromagnetic wave radiation-absorbing materials at a frequency of 8–12 GHz made of copper (Cu), nickel (Ni) and CNT with a yield of 47.5 dB shielding effectiveness (SE) [23]. [24] uses a material that absorbs electromagnetic wave radiation by combining activated carbon and iron powder (Fe) in a composite using polyvinyl alcohol. This study gives a Return Loss of –32.5 dB at a frequency of 4.65 GHz. Meanwhile, natural materials (rice husk ash) are used as an absorbent material for electromagnetic wave radiation, at a frequency of 2–18 GHz. The results of this study indicate that this material has a maximum reflection loss ability of 20 dB [25]. While using bamboo charcoal as a base material coated with NiZn<sub>2</sub>Fe<sub>2</sub>O<sub>4</sub> as an absorbent material for electromagnetic wave radiation. This research was conducted at a frequency of 2–18 GHz and 18–40 GHz. The results showed the maximum reflection loss ability of 11 dB for the frequency 2–18 GHz and a maximum of 35 dB for the frequency 18–40 GHz [26].

The use of coconut fiber as an absorbent material for electromagnetic wave radiation, at a frequency of 8–12 GHz. The results of this study indicate that the ability to apply radiation to the material or SE is a maximum of 16.35 dB [27]. Meanwhile, the use of a combination of coconut coir and charcoal powder is at a frequency of 8.2–12.4 GHz. The results of this study indicate that the ability to return loss is good at –25 dB [28]. The radiation-absorbing material uses a base material for bacterial cellulose, coated with Ni-Co. Bacterial cellulose is made into biocarbon by heating at a temperature of 1,200 °C. This research works at a frequency of 8.2–12.4 GHz. The results of this study obtained an SE value of 41.2 dB [29]. Research on radiation-absorbing materials using coconut shell as a base material. In this study, coconut shells were made into powder, then compacted and given Fe ions, and then turned into carbon by heating to a temperature of 1,000 °C. The results showed a good ability of these materials, namely with a SE of 40 dB [30].

Materials derived from nature have a good ability as a base material for absorbing electromagnetic wave radiation. Because natural ingredients contain enough cellulose to be used as a base for activated carbon. One of the materials from nature that is easy to grow and is a weed plant is water hyacinth. Research on materials that absorb electromagnetic waves from water hyacinth has never been done.

---

## 3. The aim and objectives of the study

---

The study aims to obtain EMI shielding material derived from water hyacinth and increase scientific knowledge about carbon material derived from nature (water hyacinth).

To achieve this aim, the following objectives are accomplished:

- to know the effect of water hyacinth carbonization temperature on the EMI shielding;
- to know the effect of carbonization temperature on the electrical conductivity of water hyacinth composites.

**4. Materials and methods**

**4.1. Materials**

*Water hyacinth.*

The water hyacinth used is obtained from two places, first, it comes from the Wendit Malang-Indonesia water source (free of heavy metal pollutants).

*Phenol-formaldehyde.*

The phenol-formaldehyde matrix used in this study is the production of PT. ARUKI (Arjuna Utama Kimia) – Indonesia.

**4.2. Water hyacinth activated carbon**

The parts of the water hyacinth used are the stems and leaves. The preparations made are cutting, washing and drying the water hyacinth. The drying process is carried out using an oven with a temperature of 70 °C for 4 days. Then the water hyacinth is mashed until it reaches a size of 80 mesh in powder. This is done so that the distribution of heat during the carbonization process is even.

**4.3. Carbonization**

The water hyacinth powder is placed in a tightly closed container, then put into a horizontal kiln. The carbonization process is carried out in a vacuum. The water hyacinth powder is heated from room temperature to 500 °C with a heat rise rate of 7 °C/minute. After reaching a temperature of 500 °C. Carbonization temperature variations range from 500 °C, 600 °C, 700 °C, 800 °C, 900 °C and 1,000 °C, with a heat rising speed of 3 °C/minute. After reaching the specified temperature, a holding time is then carried out for 1 hour. After that, the water hyacinth powder is cooled down to room temperature.

**4.4. Fabrication of polymer composites**

The composition of this polymer composite is 30 % water hyacinth activated carbon powder and 70 % phenol-formaldehyde (PF) resin. Then stir until evenly distributed, the mixture is then printed using a hot press with a pressure of 300 kg/cm<sup>2</sup> at a temperature of 180 °C for 10 minutes. Specimen mold dimensions=22.86×10.16×4 mm. Fig. 1 shows a schematic of polymer composite fabrication using water hyacinth activated carbon.

The steps for making a composite are as follows:

- preparation of water hyacinth powder and phenol-formaldehyde powder with a size of 200 mesh;
- mixing water hyacinth biocarbon powder with phenol-formaldehyde resin with a composition of wt 30 % water hyacinth biocarbon powder and wt 70 % phenol-formaldehyde resin. Mixing process using a ball mill;
- the mixed powder was molded by the hot press molding method with a sample size of 10.66×22.86 mm with a compacting pressure of ±200 kg/cm<sup>2</sup> at a temperature of 150 °C for 7 minutes. So that the thickness of the composite sample is ±4 mm.

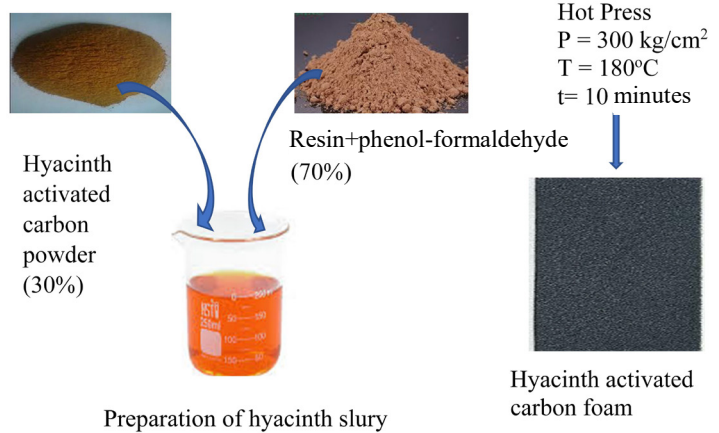


Fig. 1. Fabrication of polymer composites using water hyacinth activated carbon

**4.5. Characterization of water hyacinth activated carbon composite**

Microstructure testing of activated carbon polymer in water hyacinth using a scanning electron microscope (SEM). It uses type Zeiss Evo MA 10, which operates at 20 kV. Characterization of activated carbon crystals of water hyacinth was carried out using X-ray diffraction (XRD). It uses type X’Pert PRO (model PW3050) with monochromatic radiation and a composite testing scheme for electrical resistance and conductivity using an LCR meter as shown in Fig. 2. It is using an LCR Meter HP 4262A with a measurement frequency of 1 kHz. The SE test scheme using a Vector Network Analyzer as shown in Fig. 3.

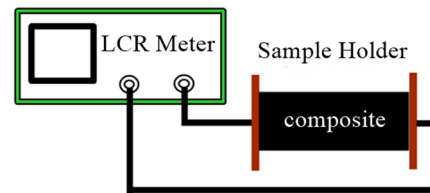


Fig. 2. Electrical conductivity test schematic

Composite samples were placed in the sample holder, then the composite resistance value was measured at a working frequency of 1 kHz.

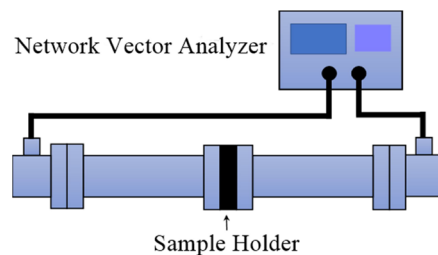


Fig. 3. Fabrication of polymer composites

The composite sample is placed on a support plate (sample holder) and placed between the transmitting antenna and the waveguide receiving antenna. VNA (Vector Network Analyzer) sends waves via the transmitter (right side

of the VNA) that will be received through the receiver on the left side of the VNA.

#### 4. 6. Electromagnetic interference (EMI) shielding effectiveness

The protection mechanism against electromagnetic wave radiation consists of reflection, absorption, and multi-reflection absorption. The Network Vector Analyzer equipment provides data on the protection capabilities of electromagnetic wave radiation from water hyacinth porous carbon material. EMI Shielding Effectiveness (SE) of a material is defined as the ratio between the power that hits the material (incident) or ( $P_I$ ) and the power that passes through the material (transmitted) or ( $P_T$ ) with the following equation [8]:

$$SE_{Total} = \left( \frac{P_I}{P_T} \right) = SE_R + SE_A + SE_M, \quad (1)$$

where  $SE_R$ ,  $SE_A$ , and  $SE_M$  are respectively SE because of reflection, absorption, and multiple reflections. When the  $SE_A$  is higher than 10 dB,  $SE_M$  is usually ignored, because the reflected waves are reabsorbed by the material. In the form of scattering parameters (S-parameters) SE.

### 5. Results of the research

#### 5. 1. SEM

The SEM test results are shown in Fig. 4.

Fig. 4, *a* shows KCl at a carbonization temperature of 500 °C spread over an irregular distance and the pores are partially open. Moreover, it shows that KCl in water hyacinth is mostly cuboid with sides 2 μm for large and 1 μm for small. Fig. 4, *b* shows the pores of water hyacinth activated carbon at 700 °C open and KCl evenly distributed in each open pore. The pore structure of water hyacinth is like a sponge. It also shows the form of KCl that sticks to the pores of water hyacinth at 700 °C. The size of KCl in water hyacinth at 700 °C is almost the same as the KCl size at 500 °C. The addition of water hyacinth carbonization temperature, which is carried out above 700 °C causes smaller pores (mesopores and micropores) to open, this is shown in Fig. 4, *c*. As is known, the pore structure of activated carbon resulting from the activation process is spread over 3 pore sizes, namely micropores (<2 nm), mesopores (2–50 nm), and macropores (>50 nm). Water hyacinth morphology is an important factor affecting composite SE.

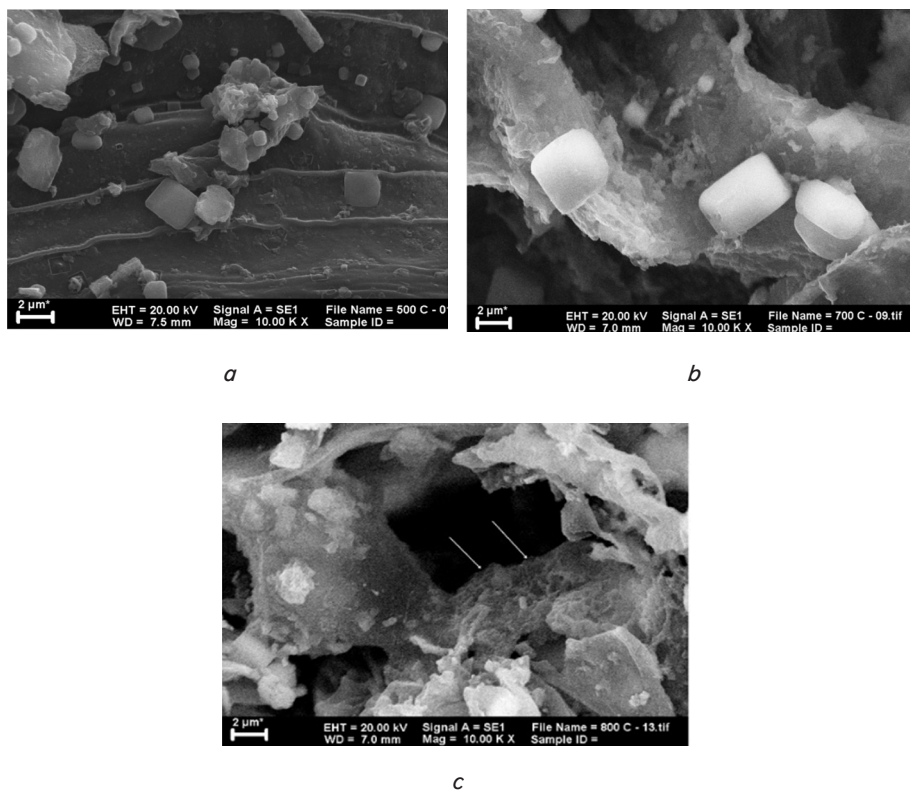


Fig. 4. SEM results of water hyacinth: *a* – carbonization temperature 500 °C; *b* – carbonization temperature 700 °C; *c* – carbonization temperature 900 °C, with a magnification of 10,000x

#### 5. 2. XRD

XRD testing is used to detect the crystalline compounds present in water hyacinth. The XRD test results are shown in Fig. 5–7.

Fig. 5–7 show the XRD patterns of water hyacinth powder with carbonization temperatures of 500 °C, 700 °C, and 900 °C. Also, KCl is at an angle of  $2\theta = 28.415^\circ$ ,  $40.62^\circ$ ,  $50.315^\circ$ ,  $58.796^\circ$ ,  $66.571^\circ$ , and  $73.910^\circ$  at all carbonization temperatures. The KCl crystal is cubic with sides of 6.2770 Å.

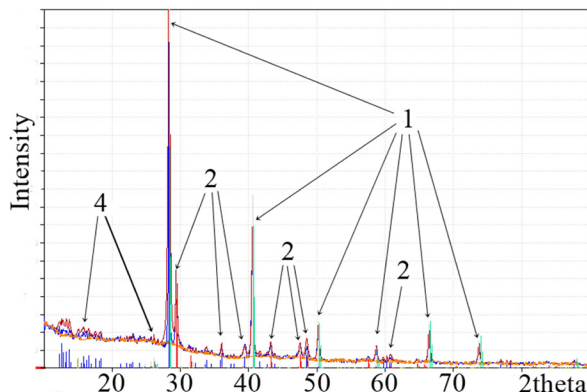


Fig. 5. XRD diffraction pattern of water hyacinth powder at a carbonization temperature of 500 °C: 1 – KCl; 2 – CaCO<sub>3</sub>; 3 – carbon; 4 – carbon graphite

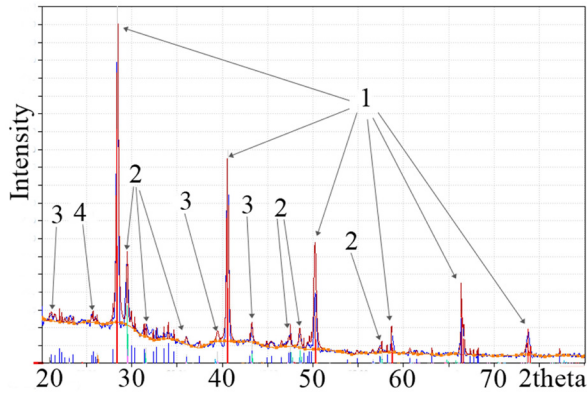


Fig. 6. XRD diffraction pattern of water hyacinth powder at a carbonization temperature of 700 °C: 1 – KCl; 2 – CaCO<sub>3</sub>; 3 – carbon; 4 – carbon graphite

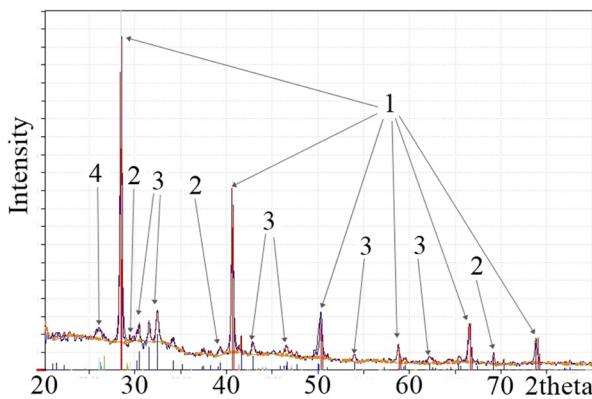


Fig. 7. XRD diffraction pattern of water hyacinth powder at a carbonization temperature of 900 °C: 1 – KCl; 2 – CaCO<sub>3</sub>; 3 – carbon; 4 – carbon graphite

### 5. 3. Electrical conductivity

Testing the electrical conductivity of the water hyacinth composite. The results of the electrical conductivity test are shown in Fig. 8.

Fig. 8 shows the relationship between the electrical conductivity of water hyacinth composites at variations in carbonization temperature. The electrical conductivity of water hyacinth composites increased with increasing carbonization temperature. It can be seen that the electrical conductivity of  $3 \cdot 10^{-7}$  S/cm at 500 °C carbonization temperature increased to  $5 \cdot 10^{-2}$  S/cm at 1,000 °C. This shows that increasing the carbonization temperature of water hyacinth gives a very good contribution to the electrical conductivity of the composite. This is because increasing the carbonization temperature increases the number of pores in the water hyacinth and improves the crystal structure of carbon. Increasing the crystal structure of carbon causes the flow of electrons in the composite to become smooth, thereby increasing the electrical conductivity of the composite. Meanwhile, electrical conductivity is one of the basic characteristics of the EMI protective material.

Testing of electromagnetic wave radiation absorption of water hyacinth composites using a VNA. The SE test results are shown in Fig. 7. In this study, the EMI performance of water hyacinth composites was measured in the frequency range of 8–12.5 GHz.

Fig. 9 shows that at the same carbonization temperature, the result is that an increase in frequency causes a decrease in the SE<sub>T</sub> value. These results illustrate that the decrease in SER is caused by the addition of the frequency value, which is greater than the addition of SE<sub>A</sub>. Whereas increasing carbonization temperature causes SE<sub>T</sub> to increase. Also, the effect of carbonization temperature on the SE<sub>T</sub> value of water hyacinth composites at a frequency of 10 GHz can be seen. The increase in value for every 100 °C of carbonization temperature is relatively the same, which is about 3 dB, except between temperatures of 600 °C and 700 °C with an increase of 7.7 dB.

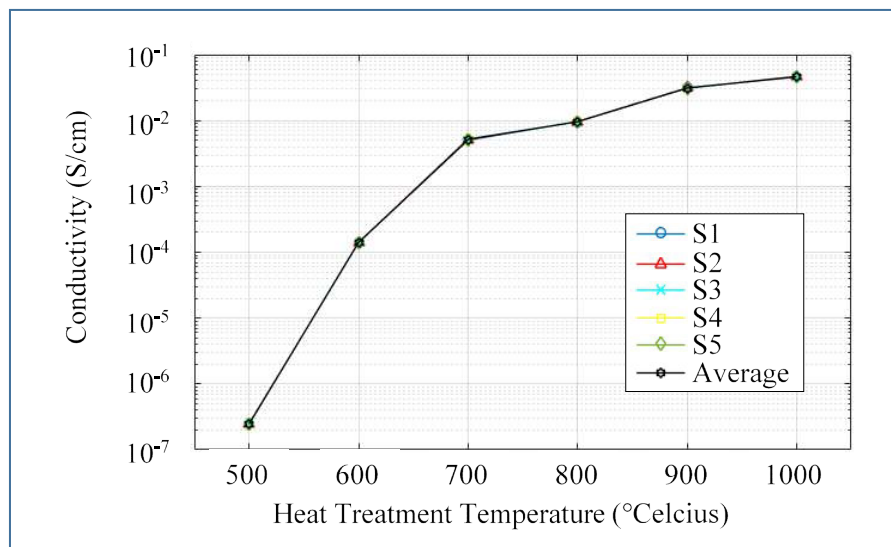


Fig. 8. Electrical conductivity of water hyacinth composites for the specimen 1 (S1) to specimen 5 (S5)

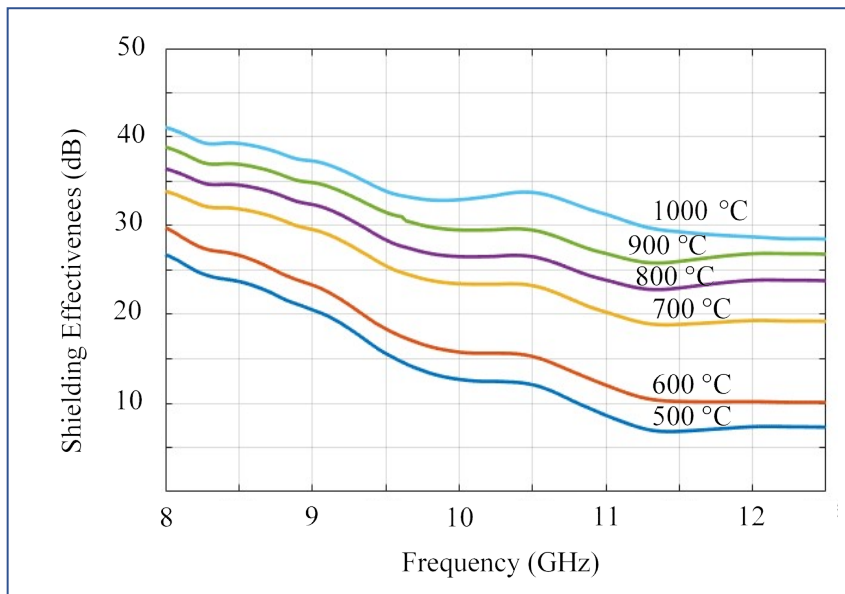


Fig. 9. EMI  $SE_T$  of water hyacinth composites at a frequency of X-band (8–12.5 GHz)

### 6. Discussion of experimental results

Based on the data that has been obtained and to better describe the EMI protection mechanism of the water hyacinth composite, a schematic of the EMI protection mechanism can be described as shown in Fig. 10.

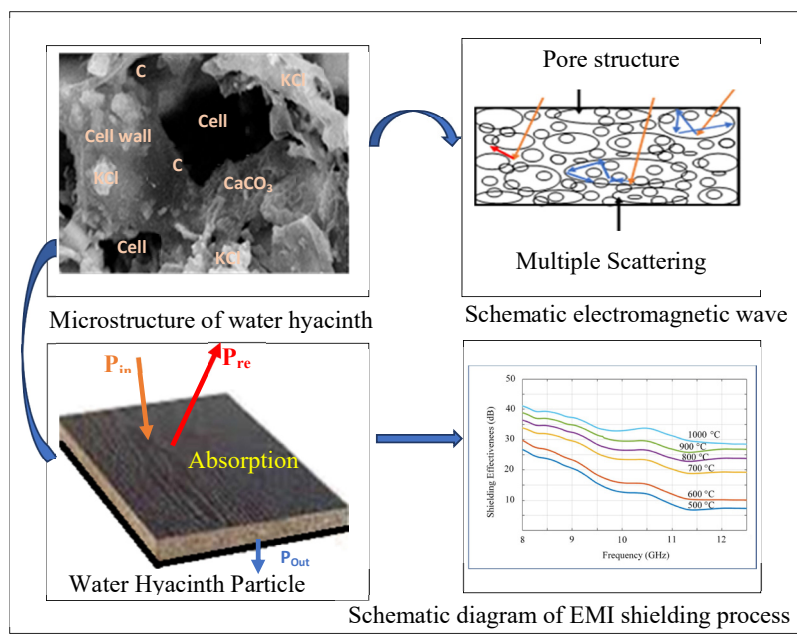


Fig. 10. Schematic of the EMI protection mechanism of a water hyacinth composite

Fig. 10 shows the ability of water hyacinth composites to absorb electromagnetic waves. This result is closely related to KCl and the pore structure in water hyacinth activated carbon, KCl in dry can't be the main absorptive element, as it is not conductive. KCl molecules are evenly distributed in water hyacinth, as shown in Fig. 4, 5. Based on Fig. 6, water hyacinth composites with a carbonization temperature of 500 °C have the lowest electrical conductivity value. However, it already has a high

$SE_T$  value of 12.7 dB (attenuation of more than 90 %). This is due to the influence of KCl that is scattered on the water hyacinth composites. When an electromagnetic wave hits KCl, the dipole ions of the KCl crystal experience an increase in the rate of dislocation motion [31] of which global concern has sharply risen due to its rapid growth. Despite ample research on its possible applications in the construction field, there are no clear references on the optimal use of the plant in finding the most efficient-use building material. In this paper, a microstructural and chemical characterization of the Water Hyacinth petiole was performed, in order to find the most efficient use as a construction material. Subsequently, two types of binder-less insulation panels were developed, with two types of particle size (pulp and staple. So it causes induced current to large. This current will be effective to weaken the penetration of electromagnetic waves.

As the electrical conductivity of water hyacinth composites increases, the pore structure begins to play a more prominent role in EMI protection performance [32]. The pore structure can increase reflection and multi-reflection in the composite thus contributing to the increase in  $SE_T$  [33]. This is indicated by a significant increase in  $SE_T$  when the carbonization temperature of water hyacinth is 700 °C.

#### 6. 1. Analysis of water hyacinth biocarbon composite

Based on Fig. 4, starting at a temperature of 500 °C (Fig. 4, a), there are only a few open pores (macropores) of water hyacinth biocarbon. At temperatures of 700 °C (Fig. 4, b) and 900 °C (Fig. 4, c), compared to (Fig. 4, a), it was shown that there were more open pores with pore diameters ranging from 7 to 9 μm, and inner pores were starting to form. At a temperature of 700 °C (Fig. 4, b), the shape of the water hyacinth biocarbon pores is shown, which are like asymmetrical corals or sponges and added inner pores are formed. At a temperature of 900 °C (Fig. 4, c) with a magnification of 10.000x, mesopores with a size of 2–50 nm are formed, there are more and deeper pores, or what can be called pores in the pores.

The higher the carbonization temperature, the more open the pores, first opening the macropores, then opening the inner pores, then opening the mesopores. The more open pores, the smaller the macropore diameter, so that at 1,000 °C the water hyacinth biocarbon temperature has a pore diameter of about 2 μm. With these pores, the water hyacinth biocarbon is very suitable as a RAM base material because when a radar electromagnetic wave hits the water hyacinth biocarbon, the wave is not reflected, but will be deflected into the pores, then it will be reflected into the water deeper pores, so the waves will break down and run out of energy.

So the wide porous water hyacinth biocarbon can increase the absorption of electromagnetic wave radiation, reduce surface reflection, improve heat dissipation of the energy absorbed. This is due to the presence of a high air volume fraction, or the absorption mechanism of multiple refractory radiation (multiple reflection). In addition, with increasing open pores, the conductivity value increases. By increasing the conductivity value, the absorption of electromagnetic wave radiation will increase.

In this study, the carbonization temperature was limited to 500–1,000 °C, using the X-band frequency (8–12.5 GHz). This research is aimed at developing anti-radar material.

**6. 2. Analysis of the electrical conductivity of composites**

The electrical conductivity of encircled composites can be analyzed based on the electric conductivity and resistivity spectrum, as seen in Fig. 11.

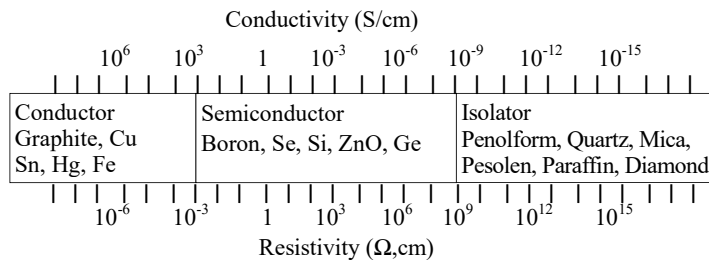


Fig. 11. Electric conductivity and resistivity spectrum

Fig. 11 shows that the higher the carbonization temperature of water hyacinth, the higher the electrical conductivity. The electrical conductivity of  $2.46 \cdot 10^{-7}$  S/cm at 500 °C increased to  $4.64 \cdot 10^{-2}$  S/cm at 1,000 °C. Because the value of electrical resistance and electrical conductivity are inversely proportional, the higher the carbonization temperature of the water hyacinth used as a composite material, the lower the electrical resistance value of the composite specimens. From a value of 22.74 MOhm at a carbonization temperature of 500 °C to 118.86 Ohm at a carbonization temperature of 1,000 °C. This shows that the carbonization temperature affects the resistance value and electrical conductivity. The increase in carbonization temperature will increase the number of carbon crystals and open the pores of water hyacinth biocarbon, so that it has an effect on decreasing the resistance value and increasing the value of the composite electrical conductivity.

Whereas the Classification of Conductive Polymer Composites Applications that depend on electrical resistivity or conductivity is described in Fig. 12.

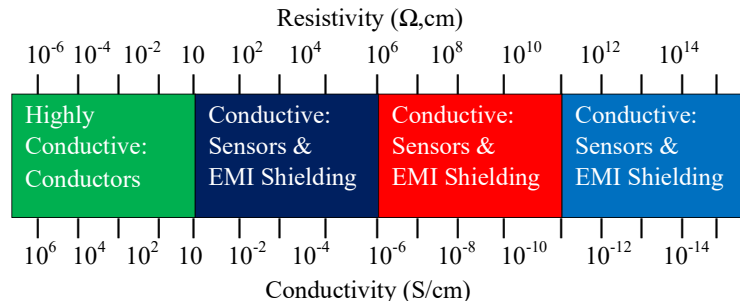


Fig. 12. Classification of Conductive Polymer Composites Applications that depend on electrical resistivity or conductivity

Based on the conductivity and electrical resistivity spectrum, the resulting water hyacinth biocarbon composite is a semiconductor material, because the electrical conductivity value of water hyacinth biocarbon composites starting with a carbonization temperature of 500 °C to 1,000 °C is between  $10^{-7}$  S/cm to  $10^{-2}$  S/cm. Whereas if based on the spectrum of Conductive Polymer Composites application in Fig. 12, the resulting water hyacinth biocarbon composite is divided into two groups, namely: water hyacinth biocarbon composite with a carbonization temperature of 500 °C is included in the dissipative electrostatic composite group because the electrical conductivity value is  $10^{-7}$  S/cm with a function as an anti-static material, while composites with carbonization temperatures ranging from 600 °C to 1,000 °C include conductive composites with functions as biosensors and Electromagnetic Interference (EMI) protection.

This research was conducted in the material conductivity range of  $100-10^{-6}$  S/cm. Materials for Electromagnetic Interference (EMI) protection were developed.

**7. Conclusions**

1. The higher the carbonization temperature, the more pores are open. The more open pores, the smaller the macro-pore diameter. So the more effective water hyacinth biocarbon as an EMI shielding material. The pore diameters range from 7 to 9 μm for 500 °C and pore diameters range from 2–50 nm for 900 °C.

2. The higher the carbonization temperature of water hyacinth, the higher the electrical conductivity. The electrical conductivity is  $2.46 \cdot 10^{-07}$  S/cm at 500 °C to  $4.64 \cdot 10^{-2}$  S/cm at 1,000 °C and the higher the carbonization temperature of the water hyacinth, the lower the electrical resistance value. From a value of 22.74 MOhm at a carbonization temperature of 500 °C to 118.86 Ohm at a carbonization temperature of 1,000 °C. This shows that the carbonization temperature affects the resistance value and electrical conductivity.

**References**

1. Basics in EMC/EMI and Power Quality Introduction, Annotations, Applications (2013). SCHAFFNER. Available at: [https://www.schaffner.com/fileadmin/media/downloads/brochure/Schaffner\\_Brochure\\_Basics\\_in\\_EMC\\_and\\_power\\_quality.pdf](https://www.schaffner.com/fileadmin/media/downloads/brochure/Schaffner_Brochure_Basics_in_EMC_and_power_quality.pdf)
2. Anzeze, A. D. (2008). Biosorption Of Heavy Metals Using Water Hyacinth Eichhornia Crassipes (Mart.) Solms- Laubach: Adsorption Properties And Technological Assessment. No. 156. Available at: [http://erepository.uonbi.ac.ke/bitstream/handle/11295/6844/Amboga\\_Biosorption%20Of%20Heavy%20Metals%20Using%20Water%20Hyacinth%20Eichhornia%20](http://erepository.uonbi.ac.ke/bitstream/handle/11295/6844/Amboga_Biosorption%20Of%20Heavy%20Metals%20Using%20Water%20Hyacinth%20Eichhornia%20)

- Crassipes%20%28Mart.%29%20Solms-%20Laubach%20%20Adsorption%20Properties%20And%20Technological%20Assessment.pdf?sequence=1&isAllowed=y
3. Jeevanandam, J., Barhoum, A., Chan, Y. S., Dufresne, A., Danquah, M. K. (2018). Review on nanoparticles and nanostructured materials: history, sources, toxicity and regulations. *Beilstein Journal of Nanotechnology*, 9, 1050–1074. doi: <https://doi.org/10.3762/bjnano.9.98>
  4. Mahmood, T., Malik, S. A., Hussain, S. T. (2010). Biosorption and recovery of heavy metals from aqueous solutions by eichhornia crassipes (water hyacinth) ASH. *BioResources*, 5 (2), 1244–1256. Available at: [https://www.researchgate.net/publication/260156524\\_Biosorption\\_and\\_recovery\\_of\\_heavy\\_metals\\_from\\_aqueous\\_solutions\\_by\\_eichhornia\\_crassipes\\_water\\_hyacinth\\_ASH](https://www.researchgate.net/publication/260156524_Biosorption_and_recovery_of_heavy_metals_from_aqueous_solutions_by_eichhornia_crassipes_water_hyacinth_ASH)
  5. Singh, A. P., Mishra, M., Dhawan, S. K. (2014). Conducting Multiphase Magnetic Nanocomposites for Microwave Shielding Application. *Nanomagnetism*, 246–277. Available at: [https://www.researchgate.net/publication/272747501\\_Conducting\\_Multiphase\\_Magnetic\\_Nanocomposites\\_for\\_Microwave\\_Shielding\\_Application](https://www.researchgate.net/publication/272747501_Conducting_Multiphase_Magnetic_Nanocomposites_for_Microwave_Shielding_Application)
  6. Wanasinghe, D., Aslani, F., Ma, G. (2020). Electromagnetic shielding properties of carbon fibre reinforced cementitious composites. *Construction and Building Materials*, 260, 120439. doi: <https://doi.org/10.1016/j.conbuildmat.2020.120439>
  7. Moradi, M., Naghdi, N., Hemmati, H., Asadi-Samani, M., Bahmani, M. (2016). Effects of the Effect of Ultra High Frequency Mobile Phone Radiation on Human Health. *Electronic Physician*, 8 (5), 2452–2457. doi: <https://doi.org/10.19082/2542>
  8. Huang, H. (2016). Development of predictive models for electromagnetic robustness of electronic components. HAL. Available at: <https://tel.archives-ouvertes.fr/tel-01261471/document>
  9. Susilo, S. H., Suparman, S., Mardiana, D., Hamidi, N. (2016). The Effect of Velocity Ratio Study on Microchannel Hydrodynamics Focused of Mixing Glycerol Nitration Reaction. *Periodica Polytechnica Mechanical Engineering*, 60 (4), 228–232. doi: <https://doi.org/10.3311/ppme.8894>
  10. Kumar, P., Narayan Maiti, U., Sikdar, A., Kumar Das, T., Kumar, A., Sudarsan, V. (2019). Recent Advances in Polymer and Polymer Composites for Electromagnetic Interference Shielding: Review and Future Prospects. *Polymer Reviews*, 59 (4), 687–738. doi: <https://doi.org/10.1080/15583724.2019.1625058>
  11. Sankaran, S., Deshmukh, K., Ahamed, M. B., Khadheer Pasha, S. K. (2018). Recent advances in electromagnetic interference shielding properties of metal and carbon filler reinforced flexible polymer composites: A review. *Composites Part A: Applied Science and Manufacturing*, 114, 49–71. doi: <https://doi.org/10.1016/j.compositesa.2018.08.006>
  12. Singh, A. K., Shishkin, A., Koppel, T., Gupta, N. (2018). A review of porous lightweight composite materials for electromagnetic interference shielding. *Composites Part B: Engineering*, 149, 188–197. doi: <https://doi.org/10.1016/j.compositesb.2018.05.027>
  13. Yousif, E., Haddad, R. (2013). Photodegradation and photostabilization of polymers, especially polystyrene: review. *SpringerPlus*, 2 (1). doi: <https://doi.org/10.1186/2193-1801-2-398>
  14. Krishnasamy, J., Thilagavathi, G., Alagirusamy, R., Das, A. (2020). Metal-embedded matrices for EMI shielding. *Materials for Potential EMI Shielding Applications*, 111–120. doi: <https://doi.org/10.1016/b978-0-12-817590-3.00007-5>
  15. Chuayjumnong, S., Karrila, S., Jumrat, S., Pianroj, Y. (2020). Activated carbon and palm oil fuel ash as microwave absorbers for microwave-assisted pyrolysis of oil palm shell waste. *RSC Advances*, 10 (53), 32058–32068. doi: <https://doi.org/10.1039/d0ra04966b>
  16. Kumar, A., Singh, D. (2015). A Review on “Weather Surveillance Radar”. *International Journal of Advanced Engineering, Management and Science (IJAEMS)*, 1 (1), 19–22.
  17. Sørensen, P. A., Kiil, S., Dam-Johansen, K., Weinell, C. E. (2009). Anticorrosive coatings: a review. *Journal of Coatings Technology and Research*, 6 (2), 135–176. doi: <https://doi.org/10.1007/s11998-008-9144-2>
  18. Hulle, A., Powar, A. (2018). Textiles as EMI Shields. *Journal of Textile Science & Engineering*, 08 (02). doi: <https://doi.org/10.4172/2165-8064.1000347>
  19. Paquin, F., Rivnay, J., Salleo, A., Stingelin, N., Silva-Acuña, C. (2015). Multi-phase microstructures drive exciton dissociation in neat semicrystalline polymeric semiconductors. *Journal of Materials Chemistry C*, 3 (41), 10715–10722. doi: <https://doi.org/10.1039/c5tc02043c>
  20. Yi, X.-S., Du, S., Zhang, L. (Eds.) (2018). *Composite materials engineering*. Vol. 2. Springer. doi: <https://doi.org/10.1007/978-981-10-5690-1>
  21. Wang, C., Murugadoss, V., Kong, J., He, Z., Mai, X., Shao, Q. et. al. (2018). Overview of carbon nanostructures and nanocomposites for electromagnetic wave shielding. *Carbon*, 140, 696–733. doi: <https://doi.org/10.1016/j.carbon.2018.09.006>
  22. Imammuddin, A. M., Soeparman, S., Suprpto, W., Sonief, A. A. (2019). Effect of Carbonization Temperature on Electrical Conductivity of Biocarbon Water Hyacinth Composites. *International Journal of Control and Automation*, 12 (9), 23–30. doi: <https://doi.org/10.33832/ijca.2019.12.9.03>
  23. Yanti, N. A. (2019). Characteristics of Biocellulose from Sago Liquid Waste with Different Ammonium Sulfate Concentration. *International Journal of Ecophysiology*, 1 (1), 56–64. doi: <https://doi.org/10.32734/ijoep.v1i1.848>



24. Idris, F. M., Hashim, M., Abbas, Z., Ismail, I., Nazlan, R., Ibrahim, I. R. (2016). Recent developments of smart electromagnetic absorbers based polymer-composites at gigahertz frequencies. *Journal of Magnetism and Magnetic Materials*, 405, 197–208. doi: <https://doi.org/10.1016/j.jmmm.2015.12.070>
25. Ribadeneyra, M. C. (2014). EMI shielding composites based on magnetic nanoparticles and nanocarbons. Universidad Carlos III de Madrid, 223. Available at: <https://core.ac.uk/download/pdf/30047274.pdf>
26. Kim, S.-Y., Kim, S.-S. (2018). Design of Radar Absorbing Structures Utilizing Carbon-Based Polymer Composites. *Polymers and Polymer Composites*, 26 (1), 105–110. doi: <https://doi.org/10.1177/096739111802600113>
27. Liu, S.-T., Chen, X.-G., Zhang, A.-B., Yan, K.-K., Ye, Y. (2014). Electromagnetic Performance of Rice Husk Ash. *BioResources*, 9 (2). doi: <https://doi.org/10.15376/biores.9.2.2328-2340>
28. Thomassin, J.-M., Jérôme, C., Pardoën, T., Bailly, C., Huynen, I., Detrembleur, C. (2013). Polymer/carbon based composites as electromagnetic interference (EMI) shielding materials. *Materials Science and Engineering: R: Reports*, 74 (7), 211–232. doi: <https://doi.org/10.1016/j.mser.2013.06.001>
29. Dai, B., Ren, Y., Wang, G., Ma, Y., Zhu, P., Li, S. (2013). Microstructure and dielectric properties of biocarbon nanofiber composites. *Nanoscale Research Letters*, 8 (1). doi: <https://doi.org/10.1186/1556-276x-8-293>
30. Pawar, S. P., Gandhi, M., Bose, S. (2016). High performance electromagnetic wave absorbers derived from PC/SAN blends containing multiwall carbon nanotubes and Fe<sub>3</sub>O<sub>4</sub> decorated onto graphene oxide sheets. *RSC Advances*, 6 (44), 37633–37645. doi: <https://doi.org/10.1039/c5ra25435c>
31. Salas-Ruiz, A., del Mar Barbero-Barrera, M., Ruiz-Tllez, T. (2019). Microstructural and Thermo-Physical Characterization of a Water Hyacinth Petiole for Thermal Insulation Particle Board Manufacture. *Materials*, 12 (4), 560. doi: <https://doi.org/10.3390/ma12040560>
32. Frederika Rumapar, K., Rumhayati, B., Triandi Tjahjanto, R. (2014). Adsorption of Lead and Copper Using Water Hyacinth Compost (*Eichornia Crassipes*). *The Journal of Pure and Applied Chemistry Research*, 3 (1), 27–34. doi: <https://doi.org/10.21776/ub.jpacr.2014.003.01.160>
33. González, M., Mokry, G., de Nicolás, M., Baselga, J., Pozuelo, J. (2016). Carbon Nanotube Composites as Electromagnetic Shielding Materials in GHz Range. *Carbon Nanotubes - Current Progress of Their Polymer Composites*. doi: <https://doi.org/10.5772/62508>